

Exploring Memorization in Adversarial Training

Yinpeng Dong¹, Ke Xu², Xiao Yang¹, Tianyu Pang¹, Zhijie Deng¹, Hang Su¹, Jun Zhu¹

¹ Dept. of Comp. Sci. & Tech., Institute for AI, BNRist Center, Tsinghua-Bosch Joint ML Center

¹ Tsinghua University, Beijing, 100084 China ² Carnegie Mellon University

{dyp17, yangxiao19, pty17, dzj17}@mails, {suhangss, dcszj}@mail}.tsinghua.edu.cn, kx1@andrew.cmu.edu

Abstract

It is well known that deep learning models have a propensity for fitting the entire training set even with random labels, which requires *memorization* of every training sample. In this paper, we investigate the memorization effect in adversarial training (AT) for promoting a deeper understanding of capacity, convergence, generalization, and especially robust overfitting of adversarially trained classifiers. We first demonstrate that deep networks have sufficient capacity to memorize adversarial examples of training data with completely random labels, but *not* all AT algorithms can converge under the extreme circumstance. Our study of AT with random labels motivates further analyses on the convergence and generalization of AT. We find that some AT methods suffer from a gradient instability issue, and the recently suggested complexity measures cannot explain robust generalization by considering models trained on random labels. Furthermore, we identify a significant drawback of memorization in AT that it could result in robust overfitting. We then propose a new mitigation algorithm motivated by detailed memorization analyses. Extensive experiments on various datasets validate the effectiveness of the proposed method.

1 Introduction

Deep neural networks (DNNs) usually exhibit excellent generalization ability in pattern recognition tasks, despite their sufficient capacity to overfit or *memorize* the entire training set with completely random labels [75]. The memorization behavior in deep learning has aroused tremendous attention to identifying the differences between learning on true and random labels [5, 48], and examining what and why DNNs memorize [21, 22, 41]. This phenomenon has also motivated a growing body of work on model capacity [5, 8], convergence [2, 20], generalization [7, 48], and other properties of DNNs, which consequently provide a better understanding of the DNN working mechanism.

In this paper, we explore the memorization behavior for a different learning algorithm — **adversarial training (AT)**. Owing to the security threat of adversarial examples, i.e., maliciously generated inputs by adding imperceptible perturbations to cause misclassification [24, 62], various defense methods have been proposed to improve the adversarial robustness of DNNs [15, 18, 38, 40, 50, 51, 66, 77]. AT is arguably the most effective defense techniques [6, 19], in which the network is trained on the adversarially augmented samples instead of the natural ones [24, 40].

Despite the popularity, the memorization behavior in AT is less explored. Schmidt et al. [58] show that a model is able to fully (over)fit the training set against an adversary, i.e., reaching almost 100% robust training accuracy, while the performance on test data is much inferior, witnessing a significant generalization gap. The overfitting phenomenon in AT is further investigated in [56]. However, it is not clear *whether DNNs could memorize adversarial examples of training data with completely random labels*. Answering this question could help to examine the effects of memorization in AT under the “extreme” circumstance and facilitate a deeper understanding of capacity, convergence, generalization, and robust overfitting of adversarially trained classifiers. In general, it is difficult for a classifier to memorize adversarial examples with random labels since the model entails a much

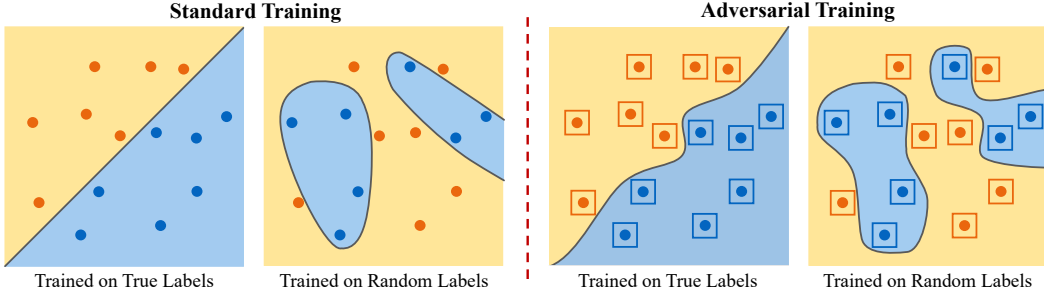


Figure 1: A conceptual illustration of decision boundaries learned via standard training and adversarial training with true and random labels, respectively. The model needs a significantly more complicated decision boundary to memorize adversarial examples of training data with random labels.

more complicated decision boundary, as illustrated in Fig. 1. Even though the network has sufficient capacity, AT may not necessarily converge. Therefore, we aim to comprehensively study this problem and explore how the analysis can motivate better algorithms.

Our contributions. We first empirically investigate the memorization behavior in AT by performing projected gradient descent based AT (**PGD-AT**) [40] and **TRADES** [77] with random labels sampled uniformly over all classes. Different from standard training (ST) that can easily memorize random labels [75], AT may *fail to converge*, with PGD-AT being a typical example. Nevertheless, we also find that TRADES can converge under this circumstance. It demonstrates that DNNs have *sufficient capacity* to memorize adversarial examples of training data even with completely random labels. This phenomenon is commonly observed on multiple datasets, network architectures, and threat models.

The memorization analysis has further implications for understanding the *convergence* and *generalization* of AT. We conduct a convergence analysis on gradient magnitude and stability to explain the counter-intuitive different convergence properties of PGD-AT and TRADES with random labels since they behave similarly when trained on true labels [56]. We corroborate that PGD-AT suffers from a gradient instability issue while the gradients of TRADES are relatively stable thanks to its adversarial loss. Moreover, by considering models trained on random labels, our generalization analysis indicates that several recently suggested complexity measures are inadequate to explain robust generalization, which is complementary to the findings in ST [32, 48, 75]. Accordingly, an appropriate explanation of robust generalization remains largely under-addressed.

Lastly, but most importantly, we identify a significant drawback of memorization in AT that it could result in *robust overfitting* [56]. We argue that the cause of robust overfitting lies in the memorization of one-hot labels in the typical AT methods. The one-hot labels can be inappropriate or even *noisy* for some adversarial examples because some data may naturally lie close to the decision boundary, and the corresponding adversarial examples should be assigned low predictive confidence [13, 61]. When the network starts to memorize these noisy examples, robust overfitting occurs, as revealed by the learning curves. To address this problem, we propose a new mitigation algorithm that impedes over-confident predictions by a regularization term for avoiding the excessive memorization of adversarial examples with possibly noisy labels. Experiments validate that our approach can eliminate robust overfitting to a large extent across multiple datasets, network architectures, threat models, and training methods, achieving better robustness under a variety of adversarial attacks than the baselines.

2 Background

2.1 Adversarial training

Adversarial training is a commonly used technique to learn robust DNN classifiers against adversarial examples. We let $\mathcal{D} = \{(\mathbf{x}_i, y_i)\}_{i=1}^n$ denote the training dataset with n samples, where $\mathbf{x}_i \in \mathbb{R}^d$ is a natural example and $y_i \in \{1, \dots, C\}$ is its true label often encoded as an one-hot vector $\mathbf{1}_{y_i}$ with totally C classes. AT can be formulated as the following robust optimization problem [40]:

$$\min_{\theta} \sum_{i=1}^n \max_{\mathbf{x}'_i \in \mathcal{S}(\mathbf{x}_i)} \mathcal{L}(f_{\theta}(\mathbf{x}'_i), y_i), \quad (1)$$

where f_{θ} is a DNN classifier with parameters θ that predicts probabilities over all classes, \mathcal{L} is the classification loss (i.e., the cross-entropy loss as $\mathcal{L}(f_{\theta}(\mathbf{x}), y) = -\mathbf{1}_y^\top \log f_{\theta}(\mathbf{x})$), and $\mathcal{S}(\mathbf{x}) = \{\mathbf{x}' : \|\mathbf{x}' - \mathbf{x}\|_p \leq \epsilon\}$ is an adversarial region centered at \mathbf{x} with radius $\epsilon > 0$ under the ℓ_p -norm threat models (e.g., ℓ_2 and ℓ_∞ norms that we consider). The robust optimization problem (1) is solved by using adversarial attacks to approximate the inner maximization and updating the model parameters θ via gradient descent. A typical method uses projected gradient descent (PGD) [40] for the inner problem, which starts at a randomly initialized point in $\mathcal{S}(\mathbf{x}_i)$ and iteratively updates the adversarial example under the ℓ_∞ -norm threat model by

$$\mathbf{x}'_i = \Pi_{\mathcal{S}(\mathbf{x}_i)}(\mathbf{x}'_i + \alpha \cdot \text{sign}(\nabla_{\mathbf{x}} \mathcal{L}(f_{\theta}(\mathbf{x}'_i), y_i))), \quad (2)$$

where $\Pi(\cdot)$ is the projection operator and α is the step size.

Besides PGD-AT, another typical and state-of-the-art method is TRADES [77], which balances the trade-off between robustness and natural accuracy by minimizing a different adversarial loss

$$\min_{\theta} \sum_{i=1}^n \left\{ \mathcal{L}(f_{\theta}(\mathbf{x}_i), y_i) + \beta \cdot \max_{\mathbf{x}'_i \in \mathcal{S}(\mathbf{x}_i)} \mathcal{D}(f_{\theta}(\mathbf{x}_i) \| f_{\theta}(\mathbf{x}'_i)) \right\}, \quad (3)$$

where \mathcal{L} is the clean cross-entropy loss on the natural example, \mathcal{D} is the Kullback–Leibler divergence, and β is a balancing hyperparameter. The inner maximization of TRADES is also solved by PGD.

Recent progress of AT includes designing new adversarial losses [18, 42, 51, 54, 65] and network architecture [70], training acceleration [59, 67, 76], and exploiting more data [1, 11, 28, 74]. A recent work highlights the training tricks in AT [52].

2.2 Related work on DNN memorization

It has been observed that DNNs can easily memorize training data with random labels [75], which requires “rethinking” of conventional techniques (e.g., VC dimension) to explain generalization. Arpit et al. [5] take a closer look at memorization and identify several qualitative differences between learning on true and random labels. Further work attempts to examine what and why DNNs memorize [21, 22, 41]. Motivated by the memorization phenomenon in deep learning, convergence of training has been analyzed in the over-parameterized setting [2, 20], while generalization has been studied with various theoretical and empirical complexity measures [4, 7, 32, 47, 48, 49].

In contrast, the memorization behavior in AT has been less explored. Previous work demonstrates that DNNs can fit training data against an adversary [40, 56, 58], e.g., achieving nearly 100% robust training accuracy against a PGD adversary, but this behavior is not explored when trained on random labels. This paper is dedicated to investigating the memorization in AT under the extreme condition with random labels, while drawing connections to capacity, convergence, generalization, and robust overfitting, with the overarching goal of better understanding the AT working mechanism.

3 Memorization in AT and implications

In this section, we first explore the memorization behavior in AT through an empirical study. Our analysis raises new questions about the convergence and generalization of AT, many of which cannot be answered by existing work. Thereafter, we provide further analytical studies on the convergence and generalization of AT by considering models trained on random labels particularly.

3.1 AT with random labels

We investigate the memorization behavior of PGD-AT [40] and TRADES [77] as two studying cases. The experiments are conducted on CIFAR-10 [35] with a Wide ResNet model [73] of depth 28 and widen factor 10 (WRN-28-10). Similar to [75], we train a network on the original dataset with true labels and on a copy of the dataset in which the true labels are corrupted by random ones. For training and robustness evaluation, a 10-step ℓ_∞ PGD adversary with $\epsilon = 8/255$ and $\alpha = 2/255$ is adopted. For TRADES, the PGD adversary maximizes the KL divergence during training, while maximizes the cross-entropy loss for robustness evaluation, as common practice [77]. We set $\beta = 6.0$. In the sequel, we denote accuracy of a classifier against the 10-step PGD adversary as “**robust accuracy**”, and accuracy on natural examples as “**natural accuracy**”.

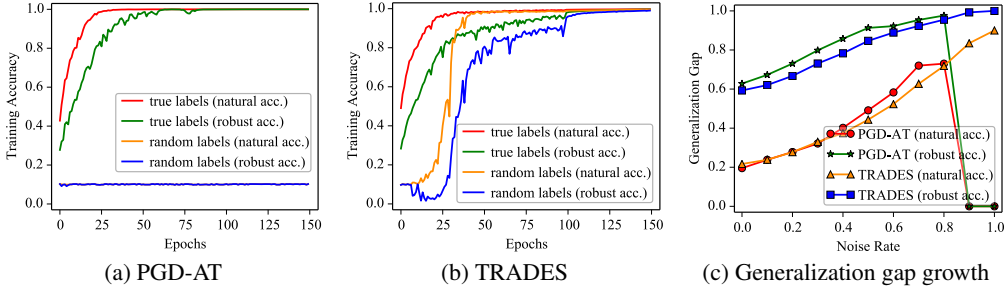


Figure 2: (a) and (b) show the natural and robust training accuracies of PGD-AT and TRADES, respectively, when trained on true or random labels. (c) shows the generalization gap under varying levels of label noise.

Fig. 2(a) and Fig. 2(b) show the learning curves of PGD-AT and TRADES, respectively, without explicit regularizations. Both methods achieve almost 100% natural and robust training accuracies when trained on true labels. When the labels are random, we observe the totally different behaviors between PGD-AT and TRADES — PGD-AT fails to converge while TRADES still reaches nearly 100% training accuracies. This phenomenon is somewhat striking because PGD-AT and TRADES are shown to perform similarly on true labels [56]. We find that the different memorization behaviors between PGD-AT and TRADES when trained on random labels can commonly be observed across a variety of datasets, model architectures, and threat models (shown in Appendix A.1, indicating that it is a general phenomenon of memorization in the two AT methods. Therefore, our finding is:

DNNs have sufficient capacity to memorize adversarial examples of training data with completely random labels, but the convergence depends on the AT algorithms.

Partially corrupted labels. We then inspect the behavior of AT under varying levels of label noise from 0% (true labels) to 100% (completely random labels). The generalization gap (i.e., difference between training and test accuracies) presented in Fig. 2(c) grows steadily as we increase the noise rate before the network fails to converge. The learning curves are provided in Appendix A.1.

Explicit regularizations. We study the role of common regularizers in AT memorization, including data augmentation, weight decay, and dropout [60]. We train TRADES on true and random labels with several combinations of regularizers. We observe that the explicit regularizers do not significantly affect the model’s ability to memorize adversarial examples, similar to the finding in ST [5, 75]. The detailed results are provided in Appendix A.1.

3.2 Convergence analysis of AT with random labels

Since we have found a counter-intuitive fact that PGD-AT and TRADES exhibit different convergence properties with random labels, it is necessary to perform a convergence analysis to understand this phenomenon. Note that our finding can hardly be explained by previous work [23, 64, 78].

We first examine the effects of different training settings on PGD-AT with random labels. We conduct experiments to analyze each training factor individually, including network architecture, attack steps, optimizer, and perturbation budget. We find that tuning the training settings fails to make PGD-AT converge with random labels (Appendix A.2 details the results). Based on the analysis, we think that the convergence issue of PGD-AT could be a result of the adversarial loss function in Eq. (1) rather than other training configurations. Specifically, TRADES in Eq. (3) minimizes a clean cross-entropy (CE) loss on natural examples, making DNNs memorize natural examples with random labels before fitting adversarial examples. As seen in Fig. 2(b), at the very early stage of TRADES training (the first 25 epochs), the natural accuracy starts to increase while the robust accuracy does not. Differently, PGD-AT in Eq. (1) directly minimizes the CE loss on adversarial examples with random labels, which can introduce unstable gradients with large variance, making it fail to converge. To corroborate the above argument, we analyze the gradient magnitude and stability below.

Gradient magnitude. First, we calculate the average gradient norm of the adversarial loss in Eq. (1) w.r.t. model parameters over each training sample for PGD-AT, and similarly calculate the average gradient norm of the clean CE loss (the first term) and the KL loss (the second term) in Eq. (3) w.r.t. parameters for TRADES to analyze their effects, respectively. We present the gradient norm along with training in Fig. 3(a). We can see that at the initial training epochs, the gradient norm of the KL

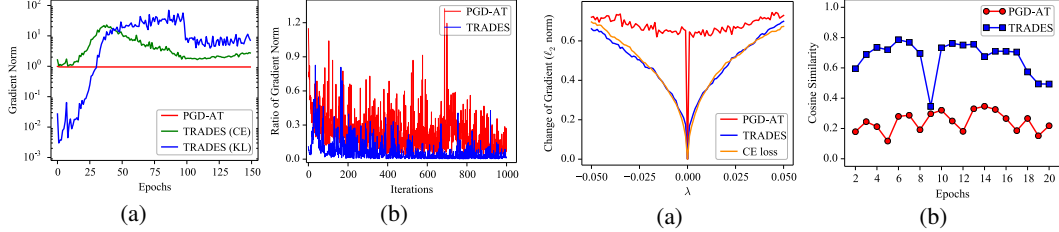


Figure 3: (a): Gradient norm of PGD-AT and TRADES along the training process. (b): The ratio of the gradient norm of PGD-AT and TRADES during the first 1000 training iterations.

Figure 4: (a): The ℓ_2 distance between the gradients at θ and $\theta + \lambda \mathbf{d}$ of different losses, where θ are initialized, $\lambda \in [-0.05, 0.05]$. (b): The cosine similarity between the gradient directions in each two successive epochs.

loss in TRADES is much smaller than that of the CE loss, which indicates that the CE loss dominates TRADES training initially. With the training progressing, the KL loss has a larger gradient norm, making the network memorize adversarial examples. However, it is still unclear why PGD-AT does not rely on a similar learning tactic for convergence. To make a direct comparison with TRADES, we rewrite the adversarial loss of PGD-AT in Eq. (1) as

$$\max_{\mathbf{x}' \in \mathcal{S}(\mathbf{x}_i)} \mathcal{L}(f_{\theta}(\mathbf{x}'_i), y_i) = \mathcal{L}(f_{\theta}(\mathbf{x}_i), y_i) + \mathcal{R}(\mathbf{x}_i, y_i, \theta),$$

where $\mathcal{R}(\mathbf{x}_i, y_i, \theta)$ denotes the difference between the CE loss on adversarial example \mathbf{x}'_i and that on natural example \mathbf{x}_i . Hence we can separately calculate the gradient norm of $\mathcal{L}(f_{\theta}(\mathbf{x}_i), y_i)$ and $\mathcal{R}(\mathbf{x}_i, y_i, \theta)$ w.r.t. parameters θ to find out the effect of $\mathcal{R}(\mathbf{x}_i, y_i, \theta)$ on training. Specifically, we measure the relative gradient magnitude, i.e., in PGD-AT we calculate the ratio of the gradient norm $\frac{\|\nabla_{\theta} \mathcal{R}(\mathbf{x}_i, y_i, \theta)\|_2}{\|\nabla_{\theta} \mathcal{L}(f_{\theta}(\mathbf{x}_i), y_i)\|_2}$; while in TRADES, we similarly calculate the ratio of the gradient norm of the KL loss to that of the CE loss. Fig. 3(b) illustrates the ratio of PGD-AT and TRADES during the first 1000 training iterations. The ratio of PGD-AT is consistently higher than that of TRADES, suggesting that $\mathcal{R}(\mathbf{x}_i, y_i, \theta)$ has a non-negligible impact on training.

Gradient stability. Then, we analyze the gradient stability, which helps to explain why PGD-AT cannot converge. We denote the adversarial loss of PGD-AT as $\mathcal{J}(\mathbf{x}, y, \theta) = \max_{\mathbf{x}' \in \mathcal{S}(\mathbf{x})} \mathcal{L}(f_{\theta}(\mathbf{x}'), y)$ with the subscript i omitted for notation simplicity. We have a theorem on gradient stability.

Theorem 1. Suppose the gradient of the clean cross-entropy loss is locally Lipschitz continuous as

$$\|\nabla_{\theta} \mathcal{L}(f_{\theta}(\mathbf{x}'), y) - \nabla_{\theta} \mathcal{L}(f_{\theta}(\mathbf{x}), y)\|_2 \leq K \|\mathbf{x}' - \mathbf{x}\|_p, \quad (4)$$

for any $\mathbf{x} \in \mathbb{R}^d$, $\mathbf{x}' \in \mathcal{S}(\mathbf{x})$, and any θ , where K is the Lipschitz constant. Then we have

$$\|\nabla_{\theta} \mathcal{J}(\mathbf{x}, y, \theta_1) - \nabla_{\theta} \mathcal{J}(\mathbf{x}, y, \theta_2)\|_2 \leq \|\nabla_{\theta} \mathcal{L}(f_{\theta_1}(\mathbf{x}), y) - \nabla_{\theta} \mathcal{L}(f_{\theta_2}(\mathbf{x}), y)\|_2 + 2\epsilon K. \quad (5)$$

We provide the proof in Appendix B, where we show the upper bound in Eq. (5) is tight. Theorem 1 indicates that the gradient of the adversarial loss $\mathcal{J}(\mathbf{x}, y, \theta)$ of PGD-AT will change more dramatically than that of the clean CE loss $\mathcal{L}(f_{\theta}(\mathbf{x}), y)$. When θ_1 and θ_2 are close, the difference between the gradients of \mathcal{L} at θ_1 and θ_2 is close to 0 due to the semi-smoothness of over-parameterized DNNs [2], but that of \mathcal{J} is relatively large due to $2\epsilon K$ in Eq. (5). To validate this, we visualize the change of gradient when moving the parameters θ along a random direction \mathbf{d} with magnitude λ . In particular, we set θ as initialization, \mathbf{d} is sampled from a Gaussian distribution and normalized filter-wise [37]. For PGD-AT and TRADES, we craft adversarial examples on-the-fly for the model with $\theta + \lambda \mathbf{d}$ and measure the change of gradient by the ℓ_2 distance to gradient at θ averaged over all data samples. The curves on gradient change of PGD-AT, TRADES, and the clean CE loss are shown in Fig. 4(a). In a small neighborhood of θ (i.e., small λ), the gradient of PGD-AT changes abruptly while the gradients of TRADES and the clean CE loss are more continuous. The gradient instability leads to a lower cosine similarity between the gradient directions w.r.t. the same data in each two successive training epochs of PGD-AT, as illustrated in Fig. 4(b). Therefore, the training of PGD-AT would be rather unstable than the gradient exhibits large variance, making it fail to converge.

Clean CE loss helps PGD-AT converge. To further verify our argument, we add the clean CE loss into the PGD-AT objective to resemble the learning of TRADES with random labels, as

$$\min_{\theta} \sum_{i=1}^n \left\{ (1 - \gamma) \cdot \mathcal{L}(f_{\theta}(\mathbf{x}_i), y_i) + \gamma \cdot \max_{\mathbf{x}' \in \mathcal{S}(\mathbf{x}_i)} \mathcal{L}(f_{\theta}(\mathbf{x}'_i), y_i) \right\}, \quad (6)$$

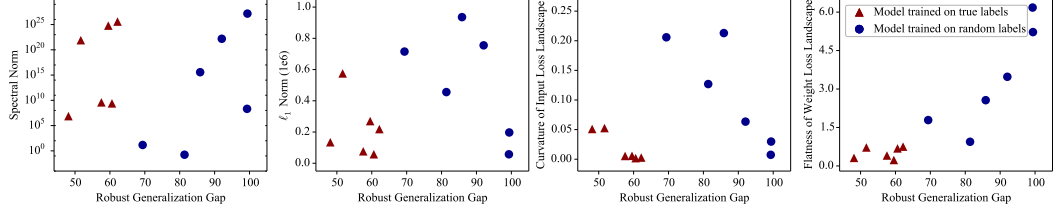


Figure 5: The results on four complexity measures of the adversarially trained models w.r.t. robust generalization gap. The training settings of these models are provided in Appendix A.3.

where γ is gradually increased from 0 to 1. By using Eq. (6), the gradient would be stabler at the initial stage, and training on random labels can successfully converge (see Fig. A.8 in Appendix A.2).

In summary, our convergence analysis identifies the gradient instability issue of PGD-AT, provides new insights on the differences between PGD-AT and TRADES, and may partially explain the failures of AT under other realistic settings beyond the scope of this section as detailed in Appendix A.2.

3.3 Generalization analysis of AT with random labels

As our study demonstrates the ability of DNNs to memorize adversarial examples with random labels, we raise the question of whether DNNs rely on a similar memorization tactic on true labels and how to explain/ensure robust generalization. Although many efforts have been devoted to studying robust generalization of AT theoretically or empirically [9, 11, 58, 63, 68, 71], they do not take the models trained on random labels into consideration. As it is easy to show that the explicit regularizations are not the adequate explanation of generalization in ST [5, 75] and AT (see Appendix A.3), people resort to some complexity measures of a model to explain generalization (i.e., a lower complexity should imply a smaller generalization gap). Here we show how the recently proposed complexity measures fail to explain robust generalization when comparing models trained on true and random labels.

We consider several norm-based and sharpness/flatness-based measures. We denote the parameters of a network by $\theta := \{W_i\}_{i=1}^m$. The norm-based measures include spectral norm $\frac{1}{\gamma_{\text{margin}}} \prod_{i=1}^m \|W_i\|_2$ and ℓ_1 norm $\frac{1}{\gamma_{\text{margin}}} \sum_{i=1}^m \|W_i\|_1$ of model parameters, where γ_{margin} is a margin on model output to make them scale-insensitive [48]. The spectral norm appears in the theoretical robust generalization bounds [63, 71] and is related to the Lipschitz constant of neural networks [14]. The ℓ_1 norm is suggested in [71] to reduce the robust generalization gap. The sharpness/flatness-based measures include the curvature of input loss landscape [43] calculated by the dominant eigenvalue of the Hessian matrix, as well as the flatness of weight loss landscape [68] related to the change of adversarial loss when moving the weights along a random direction. In Fig. 5, we plot the four complexity measures w.r.t. robust generalization gap of several models trained with various combinations of regularizations on true or random labels. It shows that these measures can hardly ensure robust generalization, that lower complexity does not necessarily imply smaller robust generalization gap, e.g., the models trained on random labels can even lead to lower complexity than those trained on true labels.

In summary, the generalization analysis indicates that the previous approaches, especially various complexity measures, cannot adequately explain and ensure the robust generalization performance in AT. Our finding of robust generalization in AT is complementary to that of standard generalization in ST [32, 48, 75]. Accordingly, robust generalization of adversarially trained models remains an open problem for future research.

4 Robust overfitting analysis

Robust overfitting has been identified as a dominant phenomenon in AT [56], i.e., shortly after the first learning rate decay, further training will continue to decrease the robust test accuracy. It further shows that several remedies for overfitting, including explicit ℓ_1 and ℓ_2 regularizations, data augmentation, etc., cannot gain improvements upon early stopping. Although robust overfitting has been thoroughly investigated, there still lacks an explanation of why it occurs. In this section, we draw a connection between memorization and robust overfitting in AT by showing that robust overfitting is caused by excessive memorization of one-hot labels in the typical AT methods. Motivated by the analysis, we then propose an effective strategy to eliminate robust overfitting.

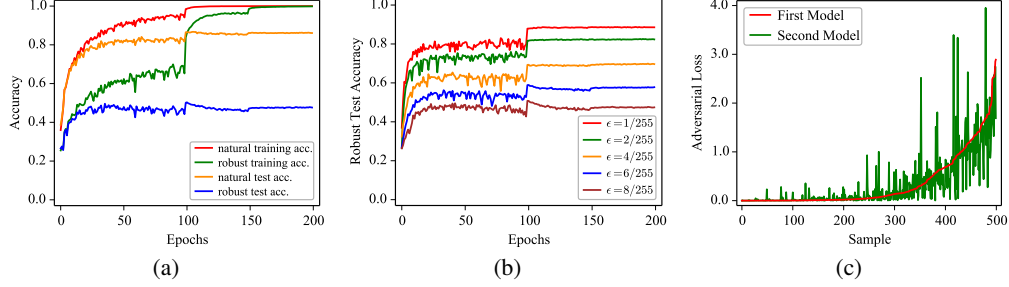


Figure 6: (a): The accuracy curves of PGD-AT with true labels to reproduce the results of robust overfitting [56]. (b): The robust test accuracy of PGD-AT under various perturbation budgets ϵ . (c): The adversarial loss of two independently trained networks by PGD-AT on 500 samples sorted by the loss of the first model.

4.1 Explaining robust overfitting

The typical AT methods (e.g., PGD-AT, TRADES, etc.) commonly adopt one-hot labels as the targets for training, as introduced in Sec. 2.1. The one-hot labels can be inappropriate for some adversarial examples because it is difficult for a network to assign high-confident one-hot labels for all perturbed samples within the perturbation budget ϵ [13, 61]. Intuitively, some examples may naturally lie close to the decision boundary and should be assigned lower predictive confidence for the corresponding worst-case adversarial examples. It indicates that the targets of some training data may be *noisy* in AT¹. After a certain epoch in training, the model starts to memorize these “hard” training examples with possibly noisy labels, leading to the degeneration of test robustness, as shown in Fig. 6(a). Thus, we hypothesize the cause of robust overfitting lies in the *memorization of one-hot labels*.

Our hypothesis is well supported by two pieces of evidence. First, we find that when the perturbation budget ϵ is small, robust overfitting does not occur, as illustrated in Fig. 6(b). This observation implies that the one-hot labels are more appropriate as the targets for adversarial examples within a smaller neighborhood while become noisier under a larger perturbation budget and lead to overfitting. Second, we validate that the “hard” training examples with higher adversarial loss values are consistent across different models. We first train two independent networks (using the same architecture and different random seeds) by PGD-AT and calculate the adversarial loss for each training sample. We show the adversarial losses on 500 samples sorted by the loss of the first model in Fig. 6(c). It can be seen that the samples with lower adversarial losses of the first model also have relatively lower losses of the second one and vice versa. We further quantitatively measure the consistency of the adversarial losses of all training samples between the two models using the Kendall’s rank coefficient [33], which is 0.85 in this case. A similar result can be observed for two different model architectures (see Appendix C.1). The results verify that the “hard” training examples with possibly noisy labels are intrinsic of a dataset, supporting our hypothesis on why robust overfitting occurs.

4.2 Mitigating robust overfitting

Based on the above analysis, we resort to the methods that are less prone to overfit noisy labels for mitigating robust overfitting in AT. Although learning with noisy labels has been broadly studied in ST [26, 31, 44, 53, 79], we find that most of these approaches are not suitable for AT. For example, a typical line of methods filter out noisy samples and train the models on the identified clean samples [26, 31, 55]. However, they will neglect a portion of training data with noisy labels, which can lead to inferior results for AT due to the reduction of sample complexity [58]².

To address this problem, we propose to regularize the predictions of adversarial examples from being over-confident by integrating the **temporal ensembling (TE)** approach [36] into the AT frameworks. TE maintains an ensemble prediction of each data and penalizes the difference between the current

¹Note that we argue the one-hot labels are noisy when used in AT, but do not argue the ground-truth labels of the dataset are noisy, which is different from previous work [57].

²We tried to adopt the *Co-teaching* approach [26] for AT, which jointly trains two models using the filtered samples given by each other. Under the experimental settings in Sec. 5, this approach achieves 51.38%/50.78% best/final accuracy under PGD-10, while PGD-AT achieves 52.64%/44.92% best/final accuracy. Though robust overfitting is alleviated by removing noisy samples, the performance is still worse than early stopping.

Table 1: Test accuracy (%) of several methods on CIFAR-10, CIFAR-100, and SVHN under the ℓ_∞ norm with $\epsilon = 8/255$ based on the ResNet-18 architecture. We choose the best checkpoint according to the highest robust accuracy on the test set under PGD-10.

Method	Natural Accuracy			PGD-10			PGD-1000			C&W-1000			AutoAttack		
	Best	Final	Diff	Best	Final	Diff	Best	Final	Diff	Best	Final	Diff	Best	Final	Diff
PGD-AT	83.75	84.82	-1.07	52.64	44.92	7.72	51.22	42.74	8.48	50.11	43.63	7.48	47.74	41.84	5.90
PGD-AT+TE	82.35	82.79	-0.44	55.79	54.83	0.96	54.65	53.30	1.35	52.30	51.73	0.57	50.59	49.62	0.97
TRADES	81.19	82.48	-1.29	53.32	50.25	3.07	52.44	48.67	3.77	49.88	48.14	1.74	49.03	46.80	2.23
TRADES+TE	83.86	83.97	-0.11	55.15	54.42	0.73	53.74	53.03	0.71	50.77	50.63	0.14	49.77	49.20	0.57

(a) The evaluation results on **CIFAR-10**.

Method	Natural Accuracy			PGD-10			PGD-1000			C&W-1000			AutoAttack		
	Best	Final	Diff	Best	Final	Diff	Best	Final	Diff	Best	Final	Diff	Best	Final	Diff
PGD-AT	57.54	57.51	0.03	29.40	21.75	7.65	28.54	20.63	7.91	27.06	21.17	5.89	24.72	19.34	5.38
PGD-AT+TE	56.45	57.12	-0.67	31.74	30.24	1.50	31.27	29.80	1.47	28.27	27.36	0.91	26.30	25.34	0.96
TRADES	57.98	56.32	1.66	29.93	27.70	2.23	29.51	26.93	2.58	25.46	24.42	1.04	24.61	23.40	1.21
TRADES+TE	59.35	58.72	0.63	31.09	30.12	0.97	30.54	29.45	1.09	26.61	25.94	0.67	25.27	24.55	0.72

(b) The evaluation results on **CIFAR-100**.

Method	Natural Accuracy			PGD-10			PGD-1000			C&W-1000			AutoAttack		
	Best	Final	Diff	Best	Final	Diff	Best	Final	Diff	Best	Final	Diff	Best	Final	Diff
PGD-AT	89.00	90.55	-1.55	54.51	46.97	7.54	52.22	42.85	9.37	48.66	44.13	4.53	46.61	38.24	8.37
PGD-AT+TE	90.09	90.91	-0.82	59.74	59.05	0.69	57.71	56.46	1.25	54.55	53.94	0.61	51.44	50.61	0.83
TRADES	90.88	91.30	-0.42	59.50	57.04	2.46	52.78	50.17	2.61	52.76	50.53	2.23	40.36	38.88	1.48
TRADES+TE	89.01	88.52	0.49	59.81	58.49	1.32	58.24	56.66	1.58	54.00	53.24	0.76	51.45	50.16	1.29

(c) The evaluation results on **SVHN**.

prediction and the ensemble prediction, which is shown to be effective for semi-supervised learning and learning with noisy labels [36]. We think that TE is suitable for AT since it enables to leverage all training samples and hinders the network from excessive memorization of one-hot labels with a regularization term. Specifically, we denote the ensemble prediction of a training sample \mathbf{x}_i as \mathbf{p}_i , which is updated in each training epoch as $\mathbf{p}_i \leftarrow \eta \cdot \mathbf{p}_i + (1 - \eta) \cdot f_\theta(\mathbf{x}_i)$, where η is the momentum term. The training objective of PGD-AT with TE can be expressed as

$$\min_{\theta} \sum_{i=1}^n \max_{\mathbf{x}'_i \in \mathcal{S}(\mathbf{x}_i)} \{ \mathcal{L}(f_\theta(\mathbf{x}'_i), y_i) + w \cdot \|f_\theta(\mathbf{x}'_i) - \hat{\mathbf{p}}_i\|_2^2 \}, \quad (7)$$

where $\hat{\mathbf{p}}_i$ is the normalization of \mathbf{p}_i as a probability vector and w is a balancing weight. TE can be similarly integrated with TRADES with the same regularization term. The network would learn to fit relatively easy samples with one-hot labels in the initial training stage, as shown in Fig. 6(a). However, after the learning rate decays, the network can keep assigning low confidence for hard samples with the regularization term in Eq. (7) and avoid fitting one-hot labels. Therefore, the proposed algorithm enables to learn under label noise in AT and alleviates the robust overfitting problem.

5 Empirical evaluation on mitigating robust overfitting

In this section, we provide the experimental results on various datasets, including CIFAR-10 [35], CIFAR-100 [35], and SVHN [46], to show the effectiveness of our proposed method on mitigating robust overfitting in AT.

Training details. We adopt the common setting that the perturbation budget is $\epsilon = 8/255$ under the ℓ_∞ norm in most experiments. We consider PGD-AT and TRADES as two typical AT baselines and integrate the proposed TE approach into them, respectively. We use the ResNet-18 [27] model as the classifier in most experiments. In training, we use the 10-step PGD adversary with $\alpha = 2/255$. The models are trained via the SGD optimizer with momentum 0.9, weight decay 0.0005, and batch size 128. For CIFAR-10/100, we set the learning rate as 0.1 initially which is decayed by 0.1 at 100 and 150 epochs with totally 200 training epochs. For SVHN, the learning rate starts from 0.01 with a

cosine annealing schedule for a total number of 80 training epochs. In our method, We set $\eta = 0.9$ and $w = 30$ along a Gaussian ramp-up curve [36].

Evaluation results. We adopt PGD-10, PGD-1000, C&W-1000 [10], and AutoAttack [17] for evaluating adversarial robustness rigorously. AutoAttack is a strong attack to evaluate model robustness, which is composed of an ensemble of diverse attacks, including APGD-CE [17], APGD-DLR [17], FAB [16], and Square attack [3]. To show the performance of robust overfitting, we report the test accuracy on the best checkpoint that achieves the highest robust test accuracy under PGD-10 and the final checkpoint, as well as the difference between these two checkpoints. The results of PGD-AT, TRADES, and the combinations of them with our proposed approach (denoted as PGD-AT+TE and TRADES+TE) on the CIFAR-10, CIFAR-100, and SVHN datasets are shown in Table 1.

We can observe that the differences between best and final test accuracies of our method are reduced to around 1%, while the accuracy gaps of PGD-AT and TRADES are much larger. It indicates that our method largely eliminates robust overfitting. Due to being less affected by robust overfitting, our method achieves higher robust accuracies than the baselines. We also show the learning curves of these methods in Fig. 7. We consistently demonstrate the effectiveness of our method on different network architectures (including WRN-34-10 and VGG-16) and threat models (including ℓ_2 norm), which will be shown in Appendix C.2.

Discussion and comparison with related work. Our method is kind of similar to the label smoothing (LS) technique, which is studied in AT [52]. Recent work has also introduced the smoothness in training labels and model weights [12, 30], which can alleviate robust overfitting to some extent. The significant difference between our work and them is that we provide a reasonable explanation for robust overfitting — *one-hot labels are noisy for AT*, while previous methods did not give such an explanation and could be viewed as solutions to our identified problem. To empirically compare with these methods, we conduct experiments on CIFAR-10 with the ResNet-18 network. Under the PGD-AT framework, we compare with the baseline PGD-AT, PGD-AT+LS, self-adaptive training (SAT) [30], and knowledge distillation with stochastic weight averaging (KD-SWA) [12]. The results under the adopted attacks are presented in Table 2. Although various techniques can alleviate robust overfitting, our method achieves better robustness than the others, validating its effectiveness.

Table 2: Test accuracy (%) of the proposed method and other methods on CIFAR-10 under the ℓ_∞ norm with $\epsilon = 8/255$ based on the ResNet-18 architecture.

Method	Natural Accuracy			PGD-10			PGD-1000			C&W-1000			AutoAttack		
	Best	Final	Diff	Best	Final	Diff	Best	Final	Diff	Best	Final	Diff	Best	Final	Diff
PGD-AT	83.75	84.82	-1.07	52.64	44.92	7.72	51.22	42.74	8.48	50.11	43.63	7.48	47.74	41.84	5.90
PGD-AT+LS	82.68	85.16	-2.48	53.70	48.90	4.80	52.56	46.31	6.25	50.41	46.06	4.35	49.02	44.39	4.63
SAT [30]	82.81	81.86	0.95	53.81	53.31	0.50	52.41	52.00	0.41	51.99	51.71	0.28	50.21	49.73	0.48
KD-SWA [12]	84.84	85.26	-0.42	54.89	53.80	1.09	53.31	52.45	0.86	51.48	50.91	0.57	50.42	49.83	0.59
PGD-AT+TE	82.35	82.79	-0.44	55.79	54.83	0.96	54.65	53.30	1.35	52.30	51.73	0.57	50.59	49.62	0.97

6 Conclusion

In this paper, we demonstrate the capacity of DNNs to fit adversarial examples with random labels by exploring memorization in adversarial training, which also poses open questions on the convergence and generalization of adversarially trained models. We corroborate that some AT methods suffer from a gradient instability issue and robust generalization can hardly be explained by complexity measures. We further identify a significant drawback of memorization in AT related to the robust overfitting phenomenon — robust overfitting is caused by memorizing one-hot labels in adversarial training. We propose a new mitigation algorithm to address this issue, with the effectiveness validated extensively.

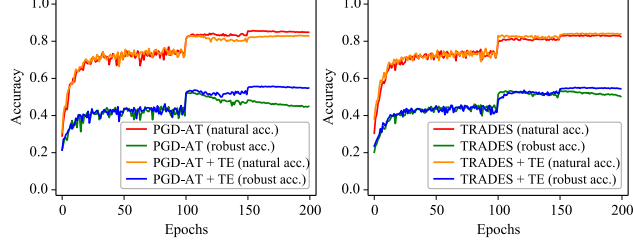


Figure 7: The natural and robust test accuracy curves (under PGD-10) of PGD-AT, TRADES, and their extensions by integrating the proposed TE approach. The models are trained on CIFAR-10 under the ℓ_∞ norm with $\epsilon = 8/255$ based on the ResNet-18 architecture.

References

- [1] Jean-Baptiste Alayrac, Jonathan Uesato, Po-Sen Huang, Alhussein Fawzi, Robert Stanforth, and Pushmeet Kohli. Are labels required for improving adversarial robustness? In *Advances in Neural Information Processing Systems (NeurIPS)*, pages 12214–12223, 2019.
- [2] Zeyuan Allen-Zhu, Yuanzhi Li, and Zhao Song. A convergence theory for deep learning via over-parameterization. In *International Conference on Machine Learning (ICML)*, pages 242–252, 2019.
- [3] Maksym Andriushchenko, Francesco Croce, Nicolas Flammarion, and Matthias Hein. Square attack: a query-efficient black-box adversarial attack via random search. In *European Conference on Computer Vision (ECCV)*, pages 484–501, 2020.
- [4] Sanjeev Arora, Rong Ge, Behnam Neyshabur, and Yi Zhang. Stronger generalization bounds for deep nets via a compression approach. In *International Conference on Machine Learning (ICML)*, pages 254–263, 2018.
- [5] Devansh Arpit, Stanisław Jastrzębski, Nicolas Ballas, David Krueger, Emmanuel Bengio, Maxinder S Kanwal, Tegan Maharaj, Asja Fischer, Aaron Courville, Yoshua Bengio, et al. A closer look at memorization in deep networks. In *International Conference on Machine Learning (ICML)*, pages 233–242, 2017.
- [6] Anish Athalye, Nicholas Carlini, and David Wagner. Obfuscated gradients give a false sense of security: Circumventing defenses to adversarial examples. In *International Conference on Machine Learning (ICML)*, pages 274–283, 2018.
- [7] Peter L Bartlett, Dylan J Foster, and Matus J Telgarsky. Spectrally-normalized margin bounds for neural networks. In *Advances in Neural Information Processing Systems (NIPS)*, pages 6240–6249, 2017.
- [8] Mikhail Belkin, Daniel Hsu, Siyuan Ma, and Soumik Mandal. Reconciling modern machine-learning practice and the classical bias–variance trade-off. *Proceedings of the National Academy of Sciences*, 116(32):15849–15854, 2019.
- [9] Sébastien Bubeck, Yin Tat Lee, Eric Price, and Ilya Razenshteyn. Adversarial examples from computational constraints. In *International Conference on Machine Learning (ICML)*, pages 831–840, 2019.
- [10] Nicholas Carlini and David Wagner. Towards evaluating the robustness of neural networks. In *IEEE Symposium on Security and Privacy (SP)*, pages 39–57, 2017.
- [11] Yair Carmon, Aditi Raghunathan, Ludwig Schmidt, Percy Liang, and John C Duchi. Unlabeled data improves adversarial robustness. In *Advances in Neural Information Processing Systems (NeurIPS)*, pages 11192–11203, 2019.
- [12] Tianlong Chen, Zhenyu Zhang, Sijia Liu, Shiyu Chang, and Zhangyang Wang. Robust overfitting may be mitigated by properly learned smoothening. In *International Conference on Learning Representations (ICLR)*, 2021.
- [13] Minhao Cheng, Qi Lei, Pin-Yu Chen, Inderjit Dhillon, and Cho-Jui Hsieh. Cat: Customized adversarial training for improved robustness. *arXiv preprint arXiv:2002.06789*, 2020.
- [14] Moustapha Cisse, Piotr Bojanowski, Edouard Grave, Yann Dauphin, and Nicolas Usunier. Parseval networks: Improving robustness to adversarial examples. In *International Conference on Machine Learning (ICML)*, pages 854–863, 2017.
- [15] Jeremy M Cohen, Elan Rosenfeld, and J Zico Kolter. Certified adversarial robustness via randomized smoothing. In *International Conference on Machine Learning (ICML)*, pages 1310–1320, 2019.
- [16] Francesco Croce and Matthias Hein. Minimally distorted adversarial examples with a fast adaptive boundary attack. In *International Conference on Machine Learning (ICML)*, pages 2196–2205, 2020.
- [17] Francesco Croce and Matthias Hein. Reliable evaluation of adversarial robustness with an ensemble of diverse parameter-free attacks. In *International Conference on Machine Learning (ICML)*, pages 2206–2216, 2020.
- [18] Yinpeng Dong, Zhijie Deng, Tianyu Pang, Jun Zhu, and Hang Su. Adversarial distributional training for robust deep learning. In *Advances in Neural Information Processing Systems (NeurIPS)*, pages 8270–8283, 2020.
- [19] Yinpeng Dong, Qi-An Fu, Xiao Yang, Tianyu Pang, Hang Su, Zihao Xiao, and Jun Zhu. Benchmarking adversarial robustness on image classification. In *Proceedings of the IEEE/CVF Conference on Computer Vision and Pattern Recognition (CVPR)*, pages 321–331, 2020.

[20] Simon Du, Jason Lee, Haochuan Li, Liwei Wang, and Xiyu Zhai. Gradient descent finds global minima of deep neural networks. In *International Conference on Machine Learning (ICML)*, pages 1675–1685, 2019.

[21] Vitaly Feldman. Does learning require memorization? a short tale about a long tail. In *Proceedings of the 52nd Annual ACM SIGACT Symposium on Theory of Computing*, pages 954–959, 2020.

[22] Vitaly Feldman and Chiyuan Zhang. What neural networks memorize and why: Discovering the long tail via influence estimation. In *Advances in Neural Information Processing Systems (NeurIPS)*, pages 2881–2891, 2020.

[23] Ruiqi Gao, Tianle Cai, Haochuan Li, Cho-Jui Hsieh, Liwei Wang, and Jason D Lee. Convergence of adversarial training in overparametrized neural networks. In *Advances in Neural Information Processing Systems (NeurIPS)*, pages 13029–13040, 2019.

[24] Ian J Goodfellow, Jonathon Shlens, and Christian Szegedy. Explaining and harnessing adversarial examples. In *International Conference on Learning Representations (ICLR)*, 2015.

[25] Sven Gowal, Chongli Qin, Jonathan Uesato, Timothy Mann, and Pushmeet Kohli. Uncovering the limits of adversarial training against norm-bounded adversarial examples. *arXiv preprint arXiv:2010.03593*, 2020.

[26] Bo Han, Quanming Yao, Xingrui Yu, Gang Niu, Miao Xu, Weihua Hu, Ivor Tsang, and Masashi Sugiyama. Co-teaching: Robust training of deep neural networks with extremely noisy labels. In *Advances in Neural Information Processing Systems (NeurIPS)*, pages 8527–8537, 2018.

[27] Kaiming He, Xiangyu Zhang, Shaoqing Ren, and Jian Sun. Deep residual learning for image recognition. In *Proceedings of the IEEE Conference on Computer Vision and Pattern Recognition (CVPR)*, pages 770–778, 2016.

[28] Dan Hendrycks, Kimin Lee, and Mantas Mazeika. Using pre-training can improve model robustness and uncertainty. In *International Conference on Machine Learning (ICML)*, pages 2712–2721, 2019.

[29] Gao Huang, Zhuang Liu, Laurens Van Der Maaten, and Kilian Q Weinberger. Densely connected convolutional networks. In *Proceedings of the IEEE Conference on Computer Vision and Pattern Recognition (CVPR)*, pages 4700–4708, 2017.

[30] Lang Huang, Chao Zhang, and Hongyang Zhang. Self-adaptive training: beyond empirical risk minimization. In *Advances in Neural Information Processing Systems (NeurIPS)*, pages 19365–19376, 2020.

[31] Lu Jiang, Zhengyuan Zhou, Thomas Leung, Li-Jia Li, and Li Fei-Fei. Mentornet: Learning data-driven curriculum for very deep neural networks on corrupted labels. In *International Conference on Machine Learning (ICML)*, pages 2304–2313, 2018.

[32] Yiding Jiang, Behnam Neyshabur, Hossein Mobahi, Dilip Krishnan, and Samy Bengio. Fantastic generalization measures and where to find them. In *International Conference on Learning Representations (ICLR)*, 2020.

[33] Maurice G Kendall. A new measure of rank correlation. *Biometrika*, 30(1/2):81–93, 1938.

[34] Diederik Kingma and Jimmy Ba. Adam: A method for stochastic optimization. In *International Conference on Learning Representations (ICLR)*, 2015.

[35] Alex Krizhevsky and Geoffrey Hinton. Learning multiple layers of features from tiny images. Technical report, University of Toronto, 2009.

[36] Samuli Laine and Timo Aila. Temporal ensembling for semi-supervised learning. In *International Conference on Learning Representations (ICLR)*, 2017.

[37] Hao Li, Zheng Xu, Gavin Taylor, Christoph Studer, and Tom Goldstein. Visualizing the loss landscape of neural nets. In *Advances in Neural Information Processing Systems (NeurIPS)*, pages 6389–6399, 2018.

[38] Fangzhou Liao, Ming Liang, Yinpeng Dong, Tianyu Pang, Xiaolin Hu, and Jun Zhu. Defense against adversarial attacks using high-level representation guided denoiser. In *Proceedings of the IEEE Conference on Computer Vision and Pattern Recognition (CVPR)*, pages 1778–1787, 2018.

[39] Chen Liu, Mathieu Salzmann, Tao Lin, Ryota Tomioka, and Sabine Süsstrunk. On the loss landscape of adversarial training: Identifying challenges and how to overcome them. In *Advances in Neural Information Processing Systems (NeurIPS)*, 2020.

[40] Aleksander Madry, Aleksandar Makelov, Ludwig Schmidt, Dimitris Tsipras, and Adrian Vladu. Towards deep learning models resistant to adversarial attacks. In *International Conference on Learning Representations (ICLR)*, 2018.

[41] Hartmut Maennel, Ibrahim Alabdulmohsin, Ilya Tolstikhin, Robert JN Baldock, Olivier Bousquet, Sylvain Gelly, and Daniel Keysers. What do neural networks learn when trained with random labels? In *Advances in Neural Information Processing Systems (NeurIPS)*, pages 19693–19704, 2020.

[42] Chengzhi Mao, Ziyuan Zhong, Junfeng Yang, Carl Vondrick, and Baishakhi Ray. Metric learning for adversarial robustness. In *Advances in Neural Information Processing Systems (NeurIPS)*, pages 480–491, 2019.

[43] Seyed-Mohsen Moosavi-Dezfooli, Alhussein Fawzi, Jonathan Uesato, and Pascal Frossard. Robustness via curvature regularization, and vice versa. In *Proceedings of the IEEE Conference on Computer Vision and Pattern Recognition (CVPR)*, pages 9078–9086, 2019.

[44] Nagarajan Natarajan, Inderjit S Dhillon, Pradeep K Ravikumar, and Ambuj Tewari. Learning with noisy labels. In *Advances in Neural Information Processing Systems (NIPS)*, pages 1196–1204, 2013.

[45] Yurii E Nesterov. A method for solving the convex programming problem with convergence rate $o(1/k^2)$. In *Dokl. akad. nauk Sssr*, volume 269, pages 543–547, 1983.

[46] Yuval Netzer, Tao Wang, Adam Coates, Alessandro Bissacco, Bo Wu, and Andrew Y Ng. Reading digits in natural images with unsupervised feature learning. In *NIPS Workshop on Deep Learning and Unsupervised Feature Learning*, 2011.

[47] Behnam Neyshabur, Ryota Tomioka, and Nathan Srebro. Norm-based capacity control in neural networks. In *Conference on Learning Theory (COLT)*, pages 1376–1401, 2015.

[48] Behnam Neyshabur, Srinadh Bhojanapalli, David McAllester, and Nati Srebro. Exploring generalization in deep learning. In *Advances in Neural Information Processing Systems (NIPS)*, pages 5947–5956, 2017.

[49] Roman Novak, Yasaman Bahri, Daniel A. Abolafia, Jeffrey Pennington, and Jascha Sohl-Dickstein. Sensitivity and generalization in neural networks: an empirical study. In *International Conference on Learning Representations (ICLR)*, 2018.

[50] Tianyu Pang, Kun Xu, Chao Du, Ning Chen, and Jun Zhu. Improving adversarial robustness via promoting ensemble diversity. In *International Conference on Machine Learning (ICML)*, pages 4970–4979, 2019.

[51] Tianyu Pang, Kun Xu, Yinpeng Dong, Chao Du, Ning Chen, and Jun Zhu. Rethinking softmax cross-entropy loss for adversarial robustness. In *International Conference on Learning Representations (ICLR)*, 2020.

[52] Tianyu Pang, Xiao Yang, Yinpeng Dong, Hang Su, and Jun Zhu. Bag of tricks for adversarial training. In *International Conference on Learning Representations (ICLR)*, 2021.

[53] Giorgio Patrini, Alessandro Rozza, Aditya Krishna Menon, Richard Nock, and Lizhen Qu. Making deep neural networks robust to label noise: A loss correction approach. In *Proceedings of the IEEE Conference on Computer Vision and Pattern Recognition (CVPR)*, pages 1944–1952, 2017.

[54] Chongli Qin, James Martens, Sven Gowal, Dilip Krishnan, Krishnamurthy Dvijotham, Alhussein Fawzi, Soham De, Robert Stanforth, and Pushmeet Kohli. Adversarial robustness through local linearization. In *Advances in Neural Information Processing Systems (NeurIPS)*, pages 13847–13856, 2019.

[55] Mengye Ren, Wenyuan Zeng, Bin Yang, and Raquel Urtasun. Learning to reweight examples for robust deep learning. In *International Conference on Machine Learning (ICML)*, pages 4334–4343, 2018.

[56] Leslie Rice, Eric Wong, and Zico Kolter. Overfitting in adversarially robust deep learning. In *International Conference on Machine Learning (ICML)*, pages 8093–8104, 2020.

[57] Amartya Sanyal, Puneet K. Dokania, Varun Kanade, and Philip Torr. How benign is benign overfitting ? In *International Conference on Learning Representations (ICLR)*, 2021.

[58] Ludwig Schmidt, Shibani Santurkar, Dimitris Tsipras, Kunal Talwar, and Aleksander Madry. Adversarially robust generalization requires more data. In *Advances in Neural Information Processing Systems (NeurIPS)*, pages 5014–5026, 2018.

[59] Ali Shafahi, Mahyar Najibi, Amin Ghiasi, Zheng Xu, John Dickerson, Christoph Studer, Larry S Davis, Gavin Taylor, and Tom Goldstein. Adversarial training for free! In *Advances in Neural Information Processing Systems (NeurIPS)*, pages 3358–3369, 2019.

[60] Nitish Srivastava, Geoffrey Hinton, Alex Krizhevsky, Ilya Sutskever, and Ruslan Salakhutdinov. Dropout: a simple way to prevent neural networks from overfitting. *The journal of machine learning research*, 15(1):1929–1958, 2014.

[61] David Stutz, Matthias Hein, and Bernt Schiele. Confidence-calibrated adversarial training: Generalizing to unseen attacks. In *International Conference on Machine Learning (ICML)*, pages 9155–9166, 2020.

[62] Christian Szegedy, Wojciech Zaremba, Ilya Sutskever, Joan Bruna, Dumitru Erhan, Ian Goodfellow, and Rob Fergus. Intriguing properties of neural networks. In *International Conference on Learning Representations (ICLR)*, 2014.

[63] Zhuozhuo Tu, Jingwei Zhang, and Dacheng Tao. Theoretical analysis of adversarial learning: A minimax approach. In *Advances in Neural Information Processing Systems (NeurIPS)*, pages 12280–12290, 2019.

[64] Yisen Wang, Xingjun Ma, James Bailey, Jinfeng Yi, Bowen Zhou, and Quanquan Gu. On the convergence and robustness of adversarial training. In *International Conference on Machine Learning (ICML)*, pages 6586–6595, 2019.

[65] Yisen Wang, Difan Zou, Jinfeng Yi, James Bailey, Xingjun Ma, and Quanquan Gu. Improving adversarial robustness requires revisiting misclassified examples. In *International Conference on Learning Representations (ICLR)*, 2020.

[66] Eric Wong and Zico Kolter. Provable defenses against adversarial examples via the convex outer adversarial polytope. In *International Conference on Machine Learning (ICML)*, pages 5286–5295, 2018.

[67] Eric Wong, Leslie Rice, and J. Zico Kolter. Fast is better than free: Revisiting adversarial training. In *International Conference on Learning Representations (ICLR)*, 2020.

[68] Dongxian Wu, Shu-Tao Xia, and Yisen Wang. Adversarial weight perturbation helps robust generalization. In *Advances in Neural Information Processing Systems (NeurIPS)*, pages 2958–2969, 2020.

[69] Cihang Xie and Alan Yuille. Intriguing properties of adversarial training. In *International Conference on Learning Representations (ICLR)*, 2020.

[70] Cihang Xie, Yuxin Wu, Laurens van der Maaten, Alan L Yuille, and Kaiming He. Feature denoising for improving adversarial robustness. In *Proceedings of the IEEE Conference on Computer Vision and Pattern Recognition (CVPR)*, pages 501–509, 2019.

[71] Dong Yin, Kannan Ramchandran, and Peter Bartlett. Rademacher complexity for adversarially robust generalization. In *International Conference on Machine Learning (ICML)*, pages 7085–7094, 2018.

[72] Fisher Yu, Dequan Wang, Evan Shelhamer, and Trevor Darrell. Deep layer aggregation. In *Proceedings of the IEEE Conference on Computer Vision and Pattern Recognition (CVPR)*, pages 2403–2412, 2018.

[73] Sergey Zagoruyko and Nikos Komodakis. Wide residual networks. In *Proceedings of the British Machine Vision Conference (BMVC)*, 2016.

[74] Runtian Zhai, Tianle Cai, Di He, Chen Dan, Kun He, John Hopcroft, and Liwei Wang. Adversarially robust generalization just requires more unlabeled data. *arXiv preprint arXiv:1906.00555*, 2019.

[75] Chiyuan Zhang, Samy Bengio, Moritz Hardt, Benjamin Recht, and Oriol Vinyals. Understanding deep learning requires rethinking generalization. In *International Conference on Learning Representations (ICLR)*, 2017.

[76] Dinghuai Zhang, Tianyuan Zhang, Yiping Lu, Zhanxing Zhu, and Bin Dong. You only propagate once: Painless adversarial training using maximal principle. In *Advances in Neural Information Processing Systems (NeurIPS)*, pages 227–238, 2019.

[77] Hongyang Zhang, Yaodong Yu, Jiantao Jiao, Eric P Xing, Laurent El Ghaoui, and Michael I Jordan. Theoretically principled trade-off between robustness and accuracy. In *International Conference on Machine Learning (ICML)*, pages 7472–7482, 2019.

[78] Yi Zhang, Orestis Plevrakis, Simon S Du, Xingguo Li, Zhao Song, and Sanjeev Arora. Over-parameterized adversarial training: An analysis overcoming the curse of dimensionality. In *Advances in Neural Information Processing Systems (NeurIPS)*, pages 679–688, 2020.

[79] Zhilu Zhang and Mert Sabuncu. Generalized cross entropy loss for training deep neural networks with noisy labels. In *Advances in Neural Information Processing Systems (NeurIPS)*, pages 8778–8788, 2018.

A Additional experiments on memorization in AT

In this section, we provide additional experiments on the memorization behavior in AT. All of the experiments are conducted on NVIDIA 2080 Ti GPUs. The source code of this paper is submitted as part of the supplementary material, and will be released after the review process.

A.1 Memorization of PGD-AT and TRADES

A.1.1 Different training settings

We first demonstrate that the different memorization behaviors between PGD-AT and TRADES can be generally observed under various settings.

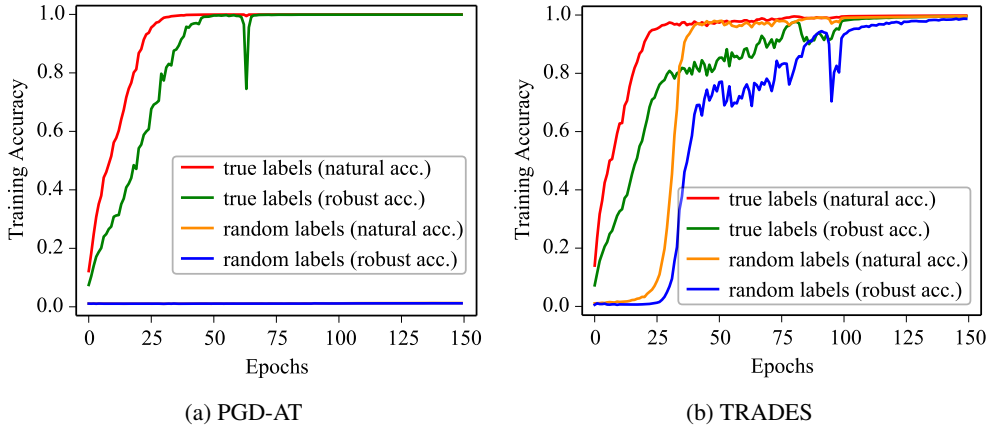


Figure A.1: The natural and robust training accuracies of PGD-AT and TRADES on CIFAR-100 when trained on true or random labels.

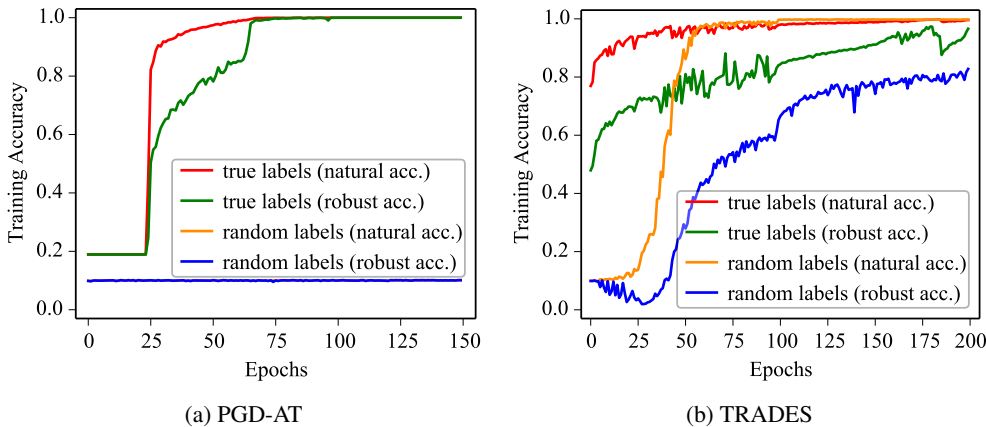


Figure A.2: The natural and robust training accuracies of PGD-AT and TRADES on SVHN when trained on true or random labels.

Datasets. Similar to Fig. 2, we show the accuracy curves of PGD-AT and TRADES when trained on true or random labels on CIFAR-100 [35] in Fig. A.1 and on SVHN [46] in Fig. A.2. We consistently observe that PGD-AT fails to converge with random labels, while TRADES can successfully converge, although it does not reach 100% accuracy on SVHN.

Model architectures. We then consider other network architectures, including the DenseNet-121 model [29] and the deep layer aggregation (DLA) model [72]. The corresponding results are shown in Fig. A.3. The similar results can be observed, although it may take more training epochs to make TRADES converge with the smaller DenseNet-121 network.

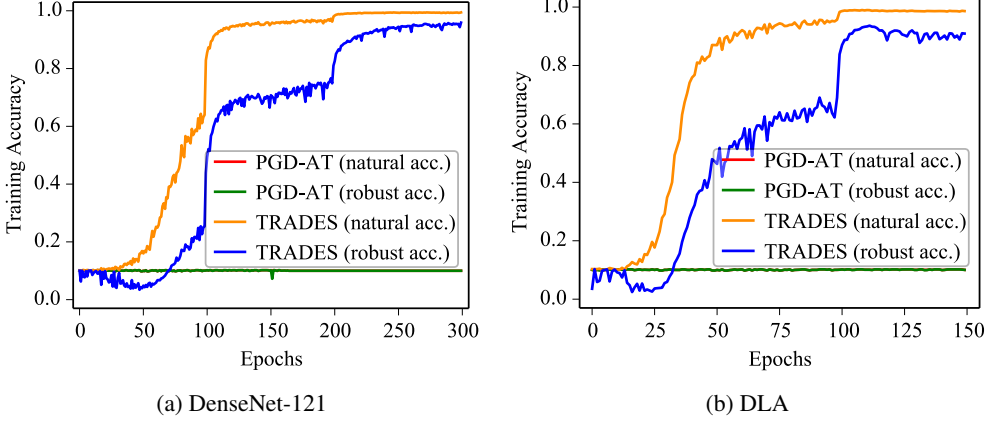


Figure A.3: The natural and robust training accuracies of PGD-AT and TRADES on CIFAR-10 with different architectures when trained on random labels.

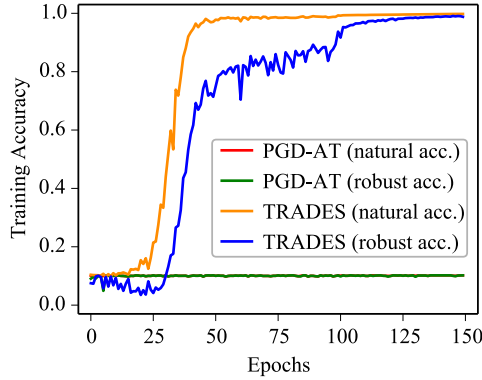


Figure A.4: The natural and robust training accuracies of PGD-AT and TRADES on CIFAR-10 under the ℓ_2 -norm threat model when trained on random labels.

Threat models. We further consider the ℓ_2 -norm threat model, in which we set $\epsilon = 1.0$ and $\alpha = 0.25$ in the 10-step PGD adversary. The learning curves of PGD-AT and TRADES are shown in Fig. A.4, which also exhibit similar results.

Perturbation budget. We study the memorization behavior in AT with different perturbation budgets ϵ . In Fig. A.5, we show that when the perturbation budget is $\epsilon = 16/255$ (ℓ_∞ norm), TRADES trained on random labels can still converge. But when we set a larger budget (e.g., $\epsilon = 32/255$), both PGD-AT and TRADES cannot obtain near 100% robust training accuracy. We also find under this condition, even AT trained on true labels cannot get 100% robust training accuracy, indicating that the gradient instability issue discussed in Sec. 3.2 results in the convergence problem.

In summary, our empirical observation that PGD-AT and TRADES perform differently when trained on random labels is general across multiple datasets, network architectures, and threat models.

A.1.2 Learning curves under different noise rates

We show the learning curves of PGD-AT and TRADES under varying levels of label noise in Fig. A.6 and Fig. A.7, respectively. In this experiment, we adopt the weight decay and data augmentation for regularizations. We can see that the network achieves maximum accuracy on the test set before fitting the noisy training set. Thus the model learns easy and simple patterns first before fitting the noise, similar to the finding in ST [5]. It can also be observed that under 80% noise rate, PGD-AT fails to converge. Note that when the noise rate is 0%, the network is trained on true labels, but the robust test accuracy also decreases after a certain epoch. This phenomenon is called robust overfitting [56], which is studied in Sec. 4.

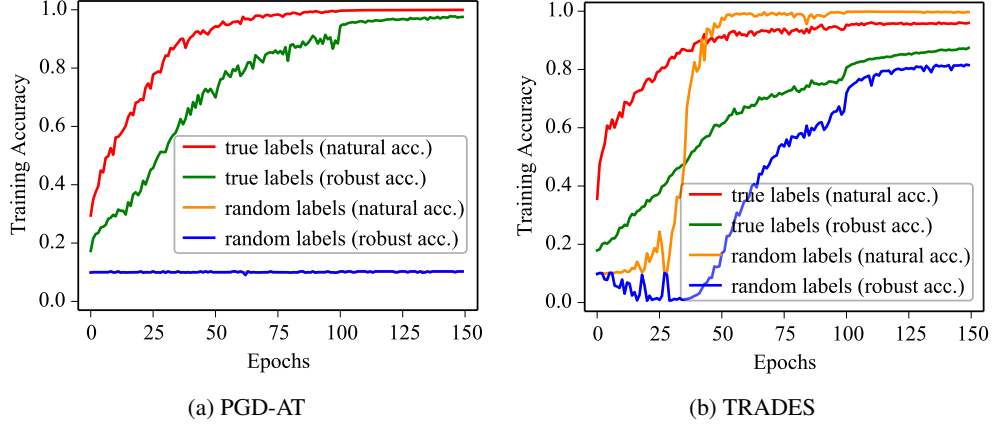


Figure A.5: The natural and robust training accuracies of PGD-AT and TRADES on CIFAR-10 with $\epsilon = 16/255$ when trained on true or random labels.

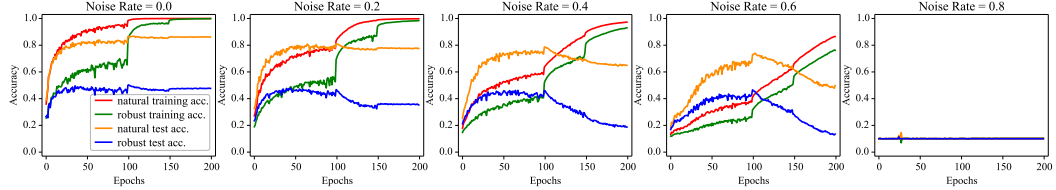


Figure A.6: Accuracy curves of PGD-AT under different noise rates on CIFAR-10.

A.1.3 Explicit regularizations

We consider three common regularizers, including data augmentation, weight decay, and dropout [60]. We train the models based on TRADES on true and random labels with several combinations of explicit regularizers. As shown in Table A.1, the explicit regularizations do not significantly affect the model’s ability to memorize adversarial examples with random labels.

Table A.1: The training accuracy, test accuracy, and generalization gap (%) of TRADES when trained on true or random labels, with and without explicit regularizations, including data augmentation (random crop and flip), weight decay (0.0002), and dropout (0.2).

Labels	Data Augmentation	Weight Decay	Dropout	Training Accuracy		Test Accuracy		Generalization Gap	
				Natural	Robust	Natural	Robust	Natural	Robust
true	✗	✗	✗	99.73	99.65	77.53	37.47	22.20	62.18
true	✓	✗	✗	99.57	97.03	82.91	45.37	16.93	51.66
true	✗	✓	✗	99.59	99.53	77.31	38.94	22.28	60.59
true	✗	✗	✓	99.65	99.40	79.96	39.86	19.69	59.54
true	✓	✓	✗	99.50	97.28	84.26	49.16	15.24	48.12
true	✗	✓	✓	99.41	99.20	80.28	41.64	19.13	57.56
random	✗	✗	✗	99.80	99.55	9.79	0.15	90.01	99.40
random	✓	✗	✗	99.36	86.10	9.71	0.24	89.65	85.86
random	✗	✓	✗	99.84	99.53	10.13	0.23	89.71	99.30
random	✗	✗	✓	99.15	92.23	9.04	0.17	90.11	92.06
random	✓	✓	✗	99.25	69.62	9.67	0.24	89.58	69.38
random	✗	✓	✓	99.38	81.57	9.54	0.19	89.84	81.38

A.2 More results on the convergence of AT

A.2.1 Training configurations

We study different training configurations on PGD-AT with random labels. We consider various factors as follows. These experiments are conducted on CIFAR-10.

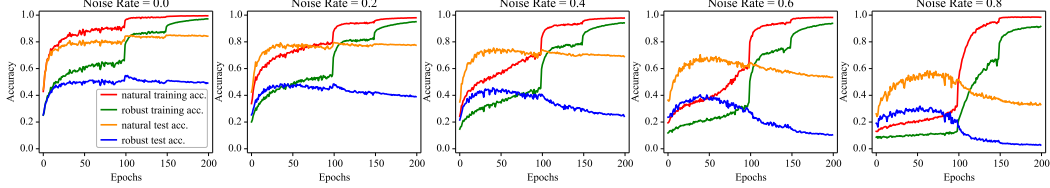


Figure A.7: Accuracy curves of TRADES under different noise rates on CIFAR-10.

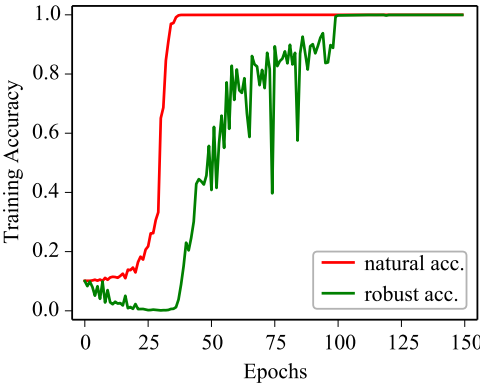


Figure A.8: The natural and robust training accuracies of the refined PGD-AT objective in Eq. (6) on CIFAR-10 when trained on random labels.

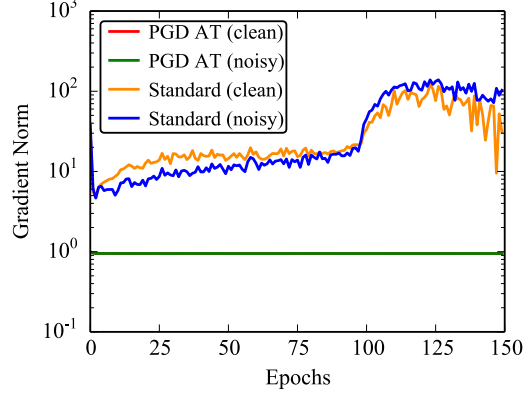


Figure A.9: The gradient norm of PGD-AT and ST given clean examples or noisy examples, when trained on 80% uniform label noise.

- **Model capacity.** Recent work suggests that model size is a critical factor to obtain better robustness [40, 69]. A possible reason why PGD-AT fails to converge with random labels may also be the insufficient model capacity. Therefore, we try to use larger models, including WRN-34-20 (which is used in [56]) and WRN-70-16 (which is used in [25]). However, using larger models under this setting cannot solve the convergence problem.
- **Attack steps.** We adopt the weaker FGSM adversary [24] for training. We also adopt the random initialization trick as argued in [67] and adjust the step size as $\alpha = 10/255$, yielding the fast adversarial training method [67]. However, fast AT still cannot converge.
- **Optimizer.** We try to use various optimizers, including the SGD momentum optimizer, the Adam optimizer [34], and the nesterov optimizer [45]; different learning rate schedules, including the piecewise decay and cosine schedules, and different learning rates (0.1 and 0.01), but none of these attempts make PGD-AT converge.
- **Perturbation budget.** The perturbation budget ϵ is an important factor to affect the convergence of PGD-AT. When ϵ approaches 0, PGD-AT would degenerate into standard training, which can easily converge [75]. Hence we try different values of ϵ , and find that PGD-AT can converge with a smaller ϵ (e.g., $\epsilon = 1/255$) but cannot converge when $\epsilon \geq 2/255$.

A.2.2 Convergence of Refined PGD-AT

Based on the convergence analysis of PGD-AT, we propose to add the clean cross-entropy loss into the adversarial loss of PGD-AT, as shown in Eq. (6). We show the learning curves of this new adversarial loss when trained on random labels on CIFAR-10 in Fig. A.8.

A.2.3 The failures of AT under realistic settings

We find that some AT methods (e.g., PGD-AT) suffer from a gradient instability issue, which results in the convergence problem when trained on random labels. Under other realistic setting, our analysis may also be valuable.

First, PGD-AT fails to converge under 80% noise rate. We think that the unstable gradients can overwhelm the useful gradients given by clean examples. To prove it, we train the models under 80%

uniform label noise, by either PGD-AT or standard training (ST) on natural examples. We then select 100 training images with wrong labels and another 100 training images with true labels for evaluation. Similarly, we calculate the gradient norm of the cross-entropy loss w.r.t. model parameters of each method. We show the results in Fig. A.9. For AT, the gradient norm of clean examples is larger than that of noisy examples at beginning, which makes the model learn to classify. However, for PGD-AT, the gradient norm of clean examples is almost the same as that of noisy examples (the two curves overlap together). And the unstable gradients provided by noisy examples would overwhelm the useful gradients given by clean examples, making the network fail to converge.

Second, when the perturbation budget is large (e.g., $\epsilon = 32/255$), AT cannot converge with true labels. This can also be explained by our convergence analysis that the gradient is very unstable with a larger perturbation budget, making it fail to converge.

A.3 More discussions on the generalization of AT

As shown in Table A.1, when trained on true labels, although the regularizers can help to reduce the generalization gap, the model without any regularization can still generalize non-trivially. The three explicit regularizations do not significantly affect the model's ability to memorize adversarial examples with random labels. In consequence, the explicit regularizers are not the adequate explanation of generalization. By inspecting the learning dynamics of AT under different noise rates in Fig. A.6 and Fig. A.7, the network achieves maximum accuracy on the test set before fitting the noisy training set, meaning that the model learns simple patterns (i.e., clean data) before memorizing the hard examples with wrong labels, similar to the observation in standard training [5]. The results suggest that optimization by itself serves as an implicit regularizer to find a model with good generalization performance.

B Proof of Theorem 1

Proof. Recall that $\mathcal{J}(\mathbf{x}, y, \boldsymbol{\theta}) = \max_{\mathbf{x}' \in \mathcal{S}(\mathbf{x})} \mathcal{L}(f_{\boldsymbol{\theta}}(\mathbf{x}'), y)$ is the adversarial loss of PGD-AT. First, we have

$$\begin{aligned}
& \|\nabla_{\boldsymbol{\theta}} \mathcal{J}(\mathbf{x}, y, \boldsymbol{\theta}_1) - \nabla_{\boldsymbol{\theta}} \mathcal{J}(\mathbf{x}, y, \boldsymbol{\theta}_2)\|_2 \\
&= \|\nabla_{\boldsymbol{\theta}} \mathcal{J}(\mathbf{x}, y, \boldsymbol{\theta}_1) - \nabla_{\boldsymbol{\theta}} \mathcal{L}(f_{\boldsymbol{\theta}_1}(\mathbf{x}), y) - \\
&\quad \nabla_{\boldsymbol{\theta}} \mathcal{J}(\mathbf{x}, y, \boldsymbol{\theta}_2) + \nabla_{\boldsymbol{\theta}} \mathcal{L}(f_{\boldsymbol{\theta}_2}(\mathbf{x}), y) + \\
&\quad \nabla_{\boldsymbol{\theta}} \mathcal{L}(f_{\boldsymbol{\theta}_1}(\mathbf{x}), y) - \nabla_{\boldsymbol{\theta}} \mathcal{L}(f_{\boldsymbol{\theta}_2}(\mathbf{x}), y)\|_2 \\
&\leq \|\nabla_{\boldsymbol{\theta}} \mathcal{J}(\mathbf{x}, y, \boldsymbol{\theta}_1) - \nabla_{\boldsymbol{\theta}} \mathcal{L}(f_{\boldsymbol{\theta}_1}(\mathbf{x}), y)\|_2 + \\
&\quad \|\nabla_{\boldsymbol{\theta}} \mathcal{J}(\mathbf{x}, y, \boldsymbol{\theta}_2) - \nabla_{\boldsymbol{\theta}} \mathcal{L}(f_{\boldsymbol{\theta}_2}(\mathbf{x}), y)\|_2 + \\
&\quad \|\nabla_{\boldsymbol{\theta}} \mathcal{L}(f_{\boldsymbol{\theta}_1}(\mathbf{x}), y) - \nabla_{\boldsymbol{\theta}} \mathcal{L}(f_{\boldsymbol{\theta}_2}(\mathbf{x}), y)\|_2.
\end{aligned} \tag{B.1}$$

From the assumption, for any $\mathbf{x} \in \mathbb{R}^d$ and $\mathbf{x}' \in \mathcal{S}(\mathbf{x})$, we have

$$\|\nabla_{\boldsymbol{\theta}} \mathcal{L}(f_{\boldsymbol{\theta}}(\mathbf{x}'), y) - \nabla_{\boldsymbol{\theta}} \mathcal{L}(f_{\boldsymbol{\theta}}(\mathbf{x}), y)\|_2 \leq K \|\mathbf{x}' - \mathbf{x}\|_p \leq \epsilon K,$$

due to the definition of $\mathcal{S}(\mathbf{x})$. We also note that $\mathcal{J}(\mathbf{x}, y, \boldsymbol{\theta})$ is the maximal cross-entropy loss \mathcal{L} within $\mathcal{S}(\mathbf{x})$, such that we have

$$\|\nabla_{\boldsymbol{\theta}} \mathcal{J}(\mathbf{x}, y, \boldsymbol{\theta}) - \nabla_{\boldsymbol{\theta}} \mathcal{L}(f_{\boldsymbol{\theta}}(\mathbf{x}), y)\|_2 \leq \epsilon K. \tag{B.2}$$

Combining Eq. (B.1) and Eq. (B.2), we can obtain Eq. (5).

Note that the bound is tight since the all the equalities can be reached. \square

Remark 1. We note that a recent work [39] gives a similar result on gradient stability. The difference is that they assume the loss function satisfies an additional Lipschitzian smoothness condition as

$$\|\nabla_{\boldsymbol{\theta}} \mathcal{L}(f_{\boldsymbol{\theta}_1}(\mathbf{x}), y) - \nabla_{\boldsymbol{\theta}} \mathcal{L}(f_{\boldsymbol{\theta}_2}(\mathbf{x}), y)\|_2 \leq K_{\boldsymbol{\theta}} \|\boldsymbol{\theta}_1 - \boldsymbol{\theta}_2\|_2,$$

where $K_{\boldsymbol{\theta}}$ is another constant. Then they prove that

$$\|\nabla_{\boldsymbol{\theta}} \mathcal{J}(\mathbf{x}, y, \boldsymbol{\theta}_1) - \nabla_{\boldsymbol{\theta}} \mathcal{J}(\mathbf{x}, y, \boldsymbol{\theta}_2)\|_2 \leq K_{\boldsymbol{\theta}} \|\boldsymbol{\theta}_1 - \boldsymbol{\theta}_2\|_2 + 2\epsilon K.$$

It can be noted that with this new assumption, we can simply obtain this result by Theorem 1. Therefore, Theorem 1 is a more general result of the previous one.

C Full experiments on robust overfitting

C.1 Additional experiments on explaining robust overfitting

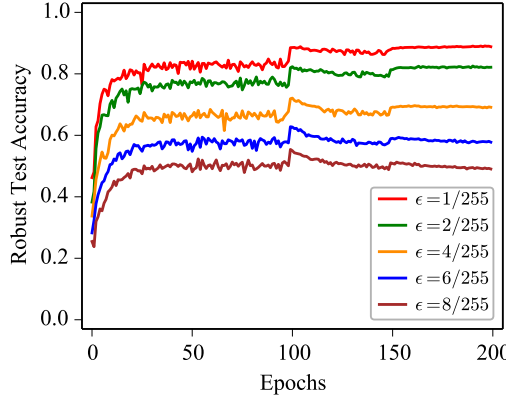


Figure C.1: The robust test accuracy of TRADES under various perturbation budgets ϵ .

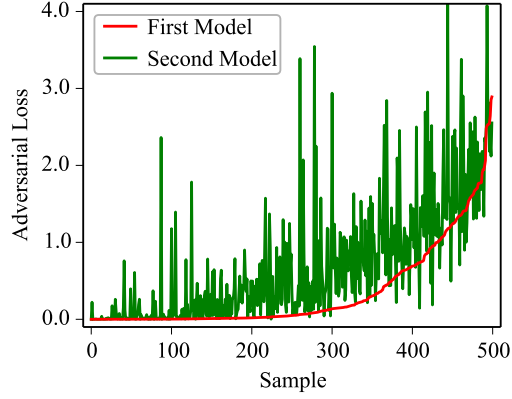


Figure C.2: The adversarial loss of WRN-28-10 and ResNet-18 trained by PGD-AT on 500 samples sorted by the loss of the first model (i.e., WRN-28-10).

First, we show the robust test accuracy curves of TRADES under various perturbation budgets in Fig. C.1. It can also be observed that when the perturbation budget is small, robust overfitting does not occur.

Second, we show that the “hard” training examples with higher adversarial loss values are consistent across different model architectures. We train one WRN-28-10 model and one ResNet-18 model based on PGD-AT. We then calculate the adversarial loss for each training sample for these two models. We show the adversarial loss on 500 samples sorted by the loss of the first model (i.e., WRN-28-10) in Fig. C.2. It can be seen that the samples with lower adversarial losses of the first model also have relatively lower losses of the second one and vice versa. The Kendall’s rank coefficient of the adversarial loss between the two models is 0.78 in this case.

C.2 Additional experiments on mitigating robust overfitting

Table C.1: Test accuracy (%) of several methods using different model architectures and threat models. We choose the best checkpoint according to the highest robust accuracy on the test set under PGD-10.

Methods	Networks	Norms	Natural Accuracy			PGD-10		
			Best	Final	Diff	Best	Final	Diff
PGD-AT	WRN-34-10		86.58	86.83	-0.25	55.83	49.52	6.31
PGD-AT+TE	WRN-34-10	ℓ_∞ ($\epsilon = 8/255$)	85.43	85.10	0.33	59.30	56.63	2.67
PGD-AT	VGG-16		79.60	81.26	-1.66	48.52	43.02	5.50
PGD-AT+TE	VGG-16		78.19	79.13	-0.94	52.06	51.29	0.77
PGD-AT			88.82	88.96	-0.14	69.05	65.96	3.09
PGD-AT+TE			87.95	88.20	-0.25	72.58	71.93	0.65
TRADES	ResNet-18	ℓ_2 ($\epsilon = 128/255$)	86.50	86.57	-0.07	70.22	66.07	4.15
TRADES+TE			88.42	88.60	-0.18	72.72	72.43	0.29

We show the results of our proposed methods on other network architectures (including WRN-34-10 and VGG-16) and threat models (including ℓ_2 norm) in Table C.1. The results consistently demonstrate the effectiveness of the proposed method.